JOURNAL of the TURKISH CHEMICAL SOCIETY
SECTION: A
CHEMISTRY

TURKISH CHEMICAL SOCIETY

# Green Preparation of *Hyphaene thebaica* Fiber Grafted Acrylic Acid for Adsorption of Pb(II) ions from Aqueous Solution

**Ahmed Salisu**[1]* **and Muhammad Saleh Salga**[1]

[1]Umaru Musa Yar' adua University, Faculty of Natural and Applied Sciences, Department of Pure and Industrial Chemistry, PMB 2218, Katsina, Nigeria.

**Abstract:** In this study, a green chemistry approach was employed in the preparation of Hyphaene thebaica fiber grafted polyacrylic acid via microwave assisted method using potassium persulfate as the chemical initiator. The optimum percentage grafting of 92% was achieved under 5 g concentration of acrylic acid, 0.2 g concentration of potassium persulfate (KPS) and 2 minutes of reaction time. The grafted sample was characterized using the following techniques, FTIR, SEM and XRD. The prepared graft copolymer was examined for adsorption of Pb(II) ions from aqueous solution in batch mode systems. The adsorption parameters such as pH, initial metal ion concentration and contact time were also studied. The Langmuir and Freundlich isotherm models were applied to simulate the equilibrium adsorption experimental data. The Langmuir model fitted well with experimental data with maximum adsorption capacity (qmax) of 20.37 mg/g at 45 minutes. Higher regression coefficient obtained confirmed the suitability of the Langmuir isotherm model which assumed monolayer coverage on the adsorbent surface. The adsorption studies revealed the efficacy of the grafted fiber for removal of Pb(II) ions from dilute aqueous solutions.

**Keywords:** *Hyphaene thebaica*, microwave, radiation, potassium persulfate, green procedures.

**Submitted:** December 21, 2018. **Accepted:** June 18, 2019.

**Cite this:** Salisu A, Salga M. Green Preparation of Hyphaene thebaica Fiber Grafted Acrylic Acid for Adsorption of Pb(II) ions from Aqueous Solution. JOTCSA. 2019;6(3):293–302.

**DOI:** https://doi.org/10.18596/jotcsa.500440.

***Corresponding author.** E-mail: (ahmed.salisu@umyu.edu.ng).

## INTRODUCTION

Cotton is by far the largest source of cellulosic fibers. Other substantial sources include; jute, sisal, flax, kenaf coir, hemp, etc. Agricultural waste biomasses such as sugarcane bagasse, rice husk, corn husk, saw-dust, orange peels, etc. are another potential large sources of ligno-cellulose. Cellulose (Figure 1) is a sustainable, less expensive, non-toxic, and biodegradable biopolymer; that has found a wide range of applications in many areas such as textile industry (1), automobile industry (2), civil engineering (3), pharmaceutical industries (4), and catalysis (5). Agricultural wastes are mostly burned after dried, thus presenting a considerable risk of pollution of the environment. Instead, proper utilization of these materials for other value added products has been the keen interest of many researchers (6). Chemical modifications of cellulose such as esterification (7), acetylation (8), etherification (9), mercerization (10) and grafting with various monomers were explored to alter the porosity and functionality of cellulose. Among these methods, grafting with various monomers present a great opportunity to tailor the physical and chemical properties of cellulose (11). Microwave irradiation initiating system for free radical polymerization reaction displays the best potential for use and fits the concept of green chemistry, i.e. less solvent consumption, shorter reaction time, energy saving, and less toxic (12). Cellulose and its derivatives have been tested for sorption of heavy metals from aqueous solutions (13, 14, 15). Pollution of surface waters has been a major ecological problem in less developed countries. Contamination of surface waters by toxic heavy metals such as Pb, Cd, As, Ni, Cr, Zn, Cu, etc. endangered humans and aquatic organisms (16). For example, lead can cause several disorders that include; renal damage, hepatic damage, central nervous system damage, and damage to the reproductive system (17). Currently, the existing conventional heavy metal wastewater treatment technologies include chemical precipitation, oxidation, evaporation, electro-deposition, chelation, ion-exchange, coagulation, membrane filtration and adsorption (18). Each of the methods has positive and negative attributes; however, adsorption has been widely reported as cheap, effective and less technical compared to other techniques (19, 20). The focus of the present study is to modify *Hyphaene thebaica* fiber, a huge lingo-cellulose agricultural waste produced in tons annually in most sub-Saharan African countries, with acrylic acid via microwave free radical graft copolymerization, characterize the graft copolymer prepared and tested for its potential for sorption of lead ions from aqueous solution.

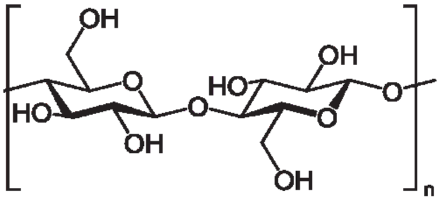

**Figure 1**: Chemical repeating unit of cellulose.

## MATERIALS AND METHODS

### Materials

Acrylic acid, acetone, methanol, and potassium persulfate (KPS) were purchased from Sigma-Aldrich (USA). $Pb(NO_3)_2$ was purchased from Loba Chemie (England). A stock solution of Pb(II) ions (1000 mg/L) was prepared by dissolving 1.599 g of $Pb(NO_3)_2$ salt in a beaker (250 mL) with deionized water. The prepared stock solution was transferred to a 1.0 liter volumetric flask, followed by the addition of 100 mL of 0.1M $HNO_3$ and made to the mark with deionized water. Desired concentrations of the metal solutions were prepared by serial dilution of the stock solution using deionized water. Other chemical reagents were of analytical grade and used as received.

### Sample Collection and Pretreatment

A fresh stalk of *Hyphaene thebaica* was collected from the local fields near Kayauki village, along Daura road Katsina State, Nigeria, in clean plastic containers. The stalk (300 g) was cleaned with distilled water, pulverized and soaked in distilled water at room temperature for 24 hrs. Thereafter the fibers were removed and washed thoroughly with distilled water and oven-dried at 50 °C. Subsequently, mercerization of the fiber was carried out with 5% (w/v) aqueous sodium hydroxide (500 mL) for 24 hours in a 1000 mL beaker at room temperature. This treatment removes lignin, wax and oil and also increases hydrophilicity (fiber wetting). The alkali treated fibers were washed thoroughly with distilled water until the pH of wash water becomes neutral. The fibers were oven dried at 50 °C.

### Graft Copolymerization of Acrylic Acid onto *Hyphaene Thebaica* Fiber

The graft copolymer was prepared using the procedure described previously (21) with minor modifications. Mercerized *Hyphaene thebaica* fiber (0.5 g) was soaked in 50 mL distilled water in a 250 mL Bomex beaker for 24 hours before graft copolymerization, in order to activate the reaction sites on the fibrous surface. Required amount of acrylic acid and KPS were added and stirred well. The reaction vessel was placed at the center of a rotating ceramic plate in the domestic microwave oven (Model WMO20L-MGSB, Skyrun, Nigeria). The reaction vessel was then exposed to microwave radiation at 900 W power for desired time. Periodically, the microwave irradiation was stopped and the reaction vessel was allowed to cool by placing it in cold water. Reaction parameters such as monomer concentration, initiator concentration and microwave exposure time were varied. Afterwards, polymeric product was precipitated by adding excess acetone and oven-dried at 50 °C. The sample was extracted by Soxhlet extraction with methanol for 6 hours to remove the homopolymer adhered to the fibrous surface. Thereafter, the prepared grafted fiber was oven-dried at 50 °C.

The percentage grafting was measured using equation (1).

$$(\%)\ \text{Grafting} = \frac{W_2 - W_1}{W_1} \times 100 \qquad \text{(Eq. 1)}$$

where $W_1$ is the initial weight of the fiber sample, $W_2$ is the weight of the grafted fiber after Soxhlet extraction (22).

### Characterization Techniques

Fourier Transform infrared analysis was performed by using a FTIR VERTEX 70/70v spectrometer (Agilent Technologies, USA). A scanning electron microscope (SEM) micrograph of the fiber and its surface morphology was examined using PHENOM PRO X (Netherlands). Powder X-ray diffraction patterns were recorded on ARL X’TRA X-ray Diffractometer (Thermo Scientific, Switzerland) using graphite monochromatic CuKα1 (1.5406 Å) and Kα2 operated at 40 kV and 30 mA in the range of 2θ angles of 5-70°.

### Batch Equilıbrium Adsorption Experiment

Batch experiments were performed by varying different variables such as pH, contact time, metal ions concentration. The experiments were carried out in 250 mL conical flasks by adding 0.1 g of the grafted fiber with 25 mL of various metal ion solution of concentrations, 20, 40, 60, 80, 100, 120, and 140 mg/L and adjusted to desired pH at room temperature using a shaker operating at 300 rpm. At desired times, the adsorption experiments were stopped, all of the 25 mL of metal ion solutions with the grafted fiber was filtered. The metal ion concentration was determined and the separated grafted fiber was placed again into the same batch and continue to the second adsorption period. All the experiments were conducted in duplicate and averages of duplicate readings were presented. The amount of Pb(II) adsorbed per unit mass of the adsorbent at equilibrium ($q_e$) (mg/g) was calculated using equation (2)

$$q_e\ (mg/g) = (c_o - c_e)\,\frac{V}{M} \qquad \text{(Eq. 2)}$$

where $c_o$ is the initial metal ions concentration (mg/L), and $c_e$ is the equilibrium concentration of metal ions in solution (mg/L), V is the volume of metal ions solution used (L) and M is the mass of the grafted fiber used (g). The equilibrium data obtained were tested using the linear forms of Langmuir isotherm model (23) and Freundlich isotherm model (24), using equation (3) and (4), respectively:

$$\frac{C_e}{q_e} = \frac{1}{q_{max}\,Q_L} + \frac{C_e}{q_m} \qquad \text{(Eq. 3)}$$

$$\mathrm{Iog}\, q_e = \mathrm{Iog}\, K_F + \frac{1}{n}\mathrm{Iog}\, C_e \qquad \text{(Eq. 4)}$$

Adsorption kinetic experimental data were modelled using two kinetic models; pseudo-first-order (25) and pseudo-second-order (26) expressed using equations (5) and (6) respectively.

$$\log(q_e - q_t) = \log q_e - \frac{k_1}{2.303}t \qquad \text{(Eq. 5)}$$

Where $q_e$and $q_t$(mg/g) are the amount of (metal ions) adsorbed at equilibrium and at time t respectively, and $k_1$(min$^{-1}$) is the equilibrium rate constant for pseudo-first-order adsorption process. The plot of log $(q_e - q_t)$ versus t gives a straight line. From the slope of the straight line, the rate constants $k_1$ were calculated. Pseudo-second-order kinetic model is expressed by the following equation:

$$\frac{t}{q_t} = \frac{1}{k_2 q_e^2} + \frac{1}{q_e}t \qquad \text{(Eq. 6)}$$

Where $q_e$ and $q_t$(mg/g) are the amount of the uptake of adsorbate at equilibrium and at time *t* respectively, and $k_2$(g/mg/min) is the equilibrium rate constant for pseudo-second order adsorption process. The slope and intercept of the plot of $\frac{t}{q_t}$ versus t can be used directly to calculate the kinetic parameters, adsorption capacity ($q_e$) and rate constant ($k_2$).

## RESULTS AND DISCUSSION

The experimental (conditions and results) of graft copolymerization reaction between the fiber and acrylic acid are presented in Table 1.

**Table 1**: Summary of results and reaction conditions of synthesis Cell-g-PAA.

| S/N | wt of fiber (g) | wt of acrylic acid (g) | wt of KPS (g) | Time (S) | % grafting |
|---|---|---|---|---|---|
| 1 | 0.5 | 5 | 0.1 | 120 | 58 |
| 2 | 0.5 | 5 | 0.2 | 120 | 92 |
| 3 | 0.5 | 5 | 0.3 | 120 | 73 |
| 4 | 0.5 | 5 | 0.4 | 120 | 43 |
| 5 | 0.5 | 2.5 | 0.2 | 180 | 7.2 |
| 6 | 0.5 | 7.5 | 0.2 | 60 | 27 |
| 7 | 0.5 | 5 | 0.5 | 120 | 39 |

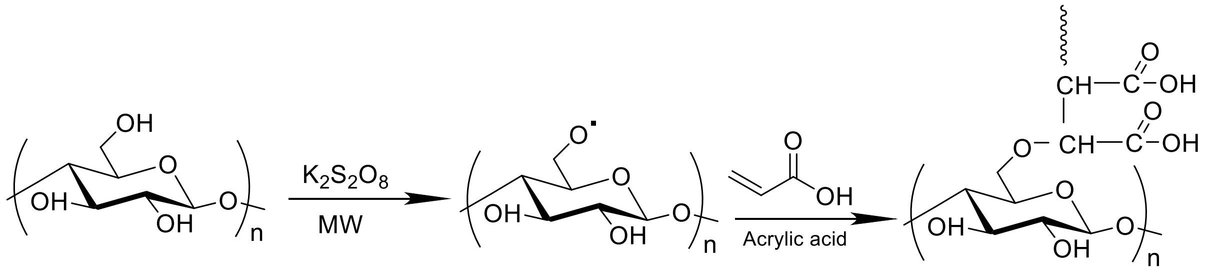

**(I)** **(II)** **(III)**

**Scheme 1:** (I) Cellulose, (II) Cellulose-macroradicals, (III) Cell-g-PAA.

A graft copolymer can be defined as a macromolecule that has branches of another polymeric species emanating from different points along its backbone (27). Different grades of graft copolymers were prepared by varying the KPS and acrylic acid concentration (Table 1). The plan of the synthesis involve optimization with regard to KPS, maintaining the acrylic acid concentration constant (i.e. S/N 1, 2, 3 & 4). Afterwards, optimization with respect to acrylic acid keeping the KPS concentration constant (i.e. S/N 5 & 6). The percentage grafting, G(%) decreased when the initiator amount was increased above 0.2g. This could be attributed to more free-radical generation that eventually may lead to premature termination (by coupling) of the growing radicals at higher concentration (16). It was observed that the highest percentage grafting was acheived at acrylic acid concentration of 5 g and KPS concentration of 0.2 g. It was also observed that the reaction reached to the optimum at a very short reaction time of 2 minutes. Microwave assisted synthesis involves synergism between microwave radiation and free radical initiator to form macroradical active sites on the cellulose backbone. Cellulose is having many –OH groups along its length, when exposed by microwave radiation in the presence of persulfate initiator. Persulfate initiator dissociates to produce a pair of persulfate ion radical ($SO_4^{2-}\cdot$). These radicals may abstract H-atom from the easily accessible (–OH) group (28). This would form active sites on the cellulose backbone (macroradicals), this would eventually initiate graft copolymerization on contact with acrylic acid. The plausible mechanism of the reaction is shown in Scheme 1.

## Characterization of The Grafted Fiber

### *FTIR Analysis*

FTIR spectrum of the mercerized fiber is shown in Figure 2. The broad absorption peak at 3335 cm$^{-1}$ was attributed O-H stretching vibrations of cellulose and the absorption peak at 2888 cm$^{-1}$ was assigned to C-H stretching vibration. The peak at 1026 cm$^{-1}$ was attributed to stretching C-O of β-glucosidic linkage of pyranose ring (29). Meanwhile in the spectrum of the grafted fiber (Figure 3), an additional sharp absorption peak at 1707 cm$^{-1}$ indicates the C=O stretching vibration of carboxylic acid functional group, this confirmed that the polyacrylic acid had been successfully grafted onto the surface of the fiber.

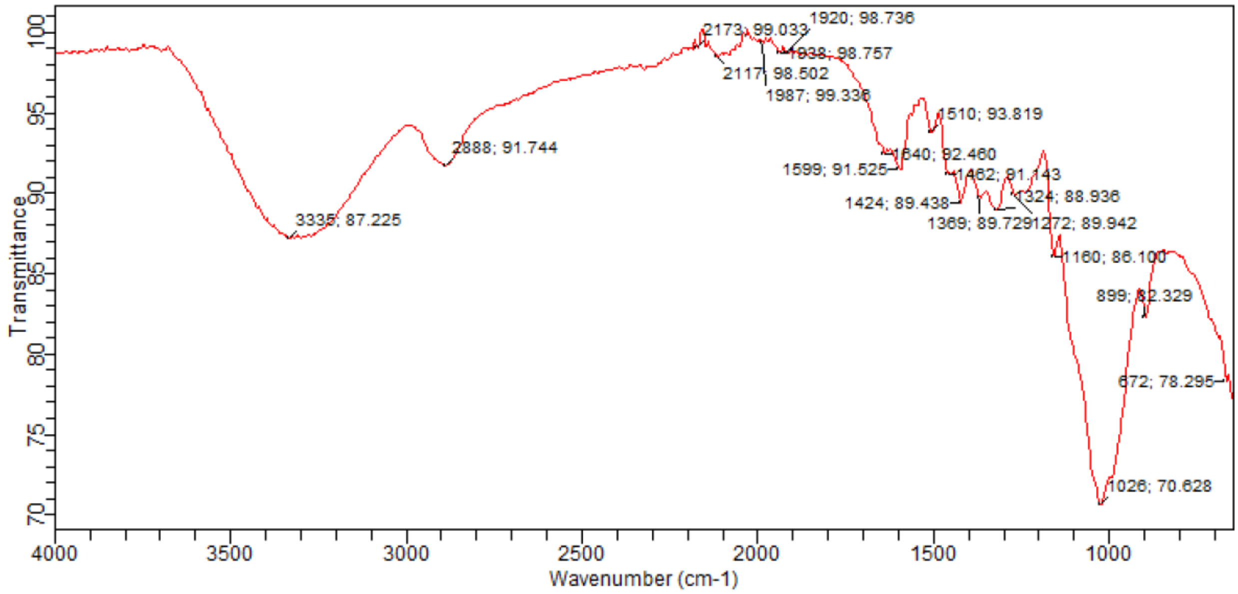

**Figure 2:** FTIR spectrum of the mercerized fiber.

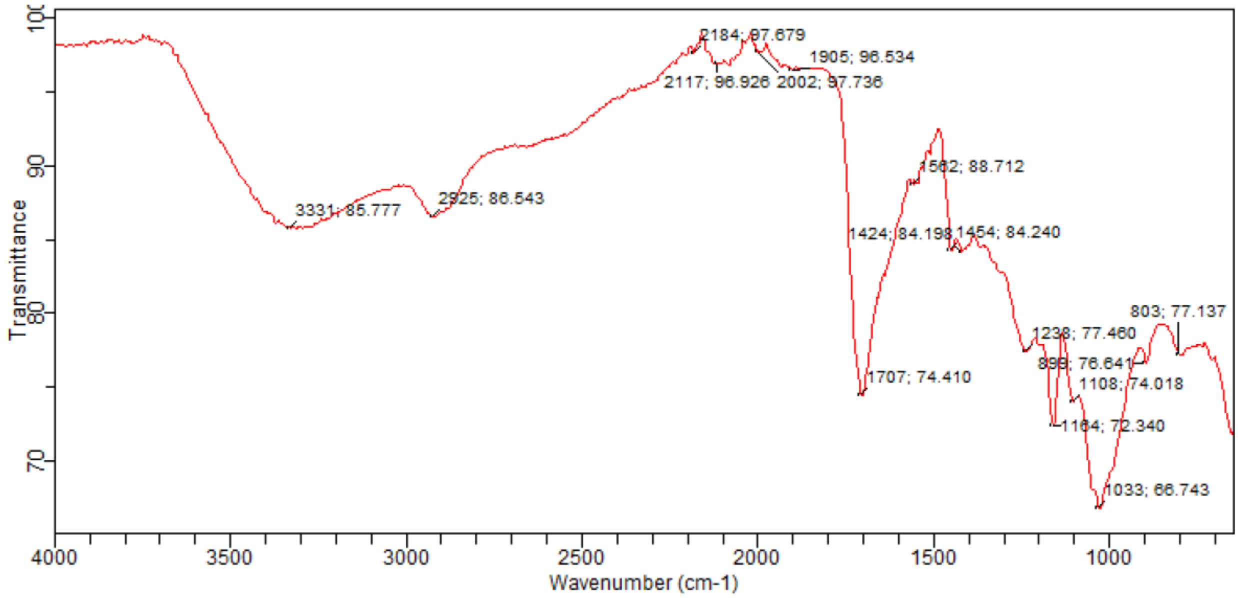

**Figure 3:** FTIR spectrum of the grafted fiber (Cell-g-PAA).

### *XRD Analysis*

The XRD pattern of mercerized and grafted fiber was presented in Figure 4. The characteristic peaks of mercerized fiber were observed at 22.13° and 14.3° (2θ degree) with relative intensities of 1056 and 606, respectively. The peaks of grafted sample were found at 20.25° and 16.1° (2θ degree) with relative intensities of 806.2 and 509.5, respectively. This showed that grafting has resulted in the decrease in the peak intensity of grafted sample. It was observed that the grafting of polyacrylic acid onto the backbone of the fiber changed most of the crystalline phase to amorphous phase (30).

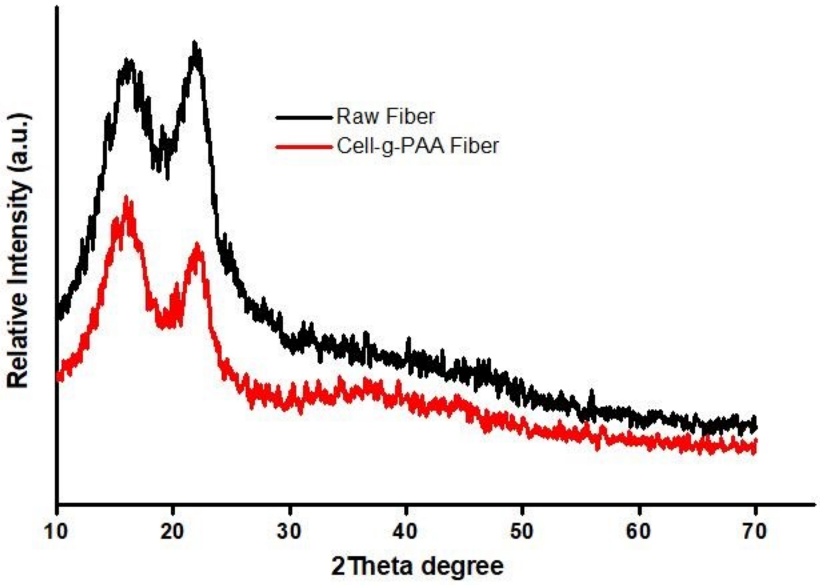

**Figure 4:** X-ray diffractogram of mercerized fiber and grafted fiber (Cell-g-PAA).

### *Scanning Electron Microscopy (SEM)*

Surface morphology of mercerized fiber and the grafted fiber were examined using a scanning electron microscope. The SEM images of mercerized and grafted fiber were shown in Figure 5a and 5b, respectively. The SEM images were taken at the same magnification for a suitable comparison of morphological changes that occured. It is clearly seen that the mercerized fiber was smooth after mercerization which removed lignin lipids and waxes. It can be observed that a substantial amount of polyacrylic acid was left behind on the surface of the grafted fiber after Soxhlet extraction that removed the homopolymer that is unreacted with the fiber. This has confirmed the grafting of polyacrylic acid onto the surface of the fiber.

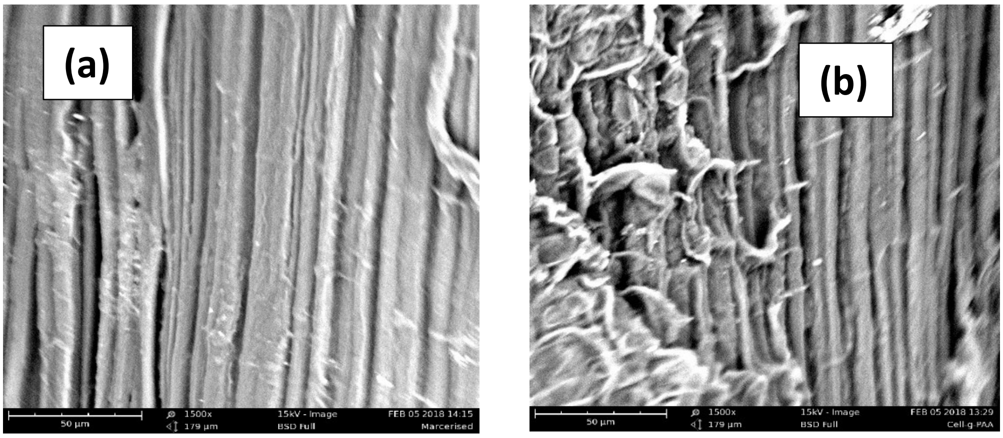

**Figure 5:** SEM images of (a) mercerized fiber and (b) grafted fiber (Cell-g-PAA).

## BATCH ADSORPTION STUDY

### Effect of pH of the Solution

In order to examine the influence of this important parameter on the adsorption of Pb(II), the experiments were conducted in the pH range of pH 2.0-9.0. The adsorption capacity for different values of pH is represented in Figure 6. The maximum adsorption capacity of Pb(II) takes place at pH 5.0 and decreased afterwards. At low pH values, there is a greater competition between protons and metal ions which may eventually be protonated most of the adsorption sites on the adsorbent surface, resulting in low adsorption capacity because of electrostatic repulsion. With the increase of pH from 6.0-8.0, the carboxyl groups (-COOH) in polyacrylic acid and hydroxyl groups in cellulose (-OH) become free from protonation due to the diminishing of hydrogen ion concentration, resulting in the decreased in competition of protons with Pb(II) ions for adsorption sites and subsequently good adsorption capacities were also observed. However the precipitation of Pb(II) may predominates over adsorption at pH values above pH 9.0 that is why they are not considered.

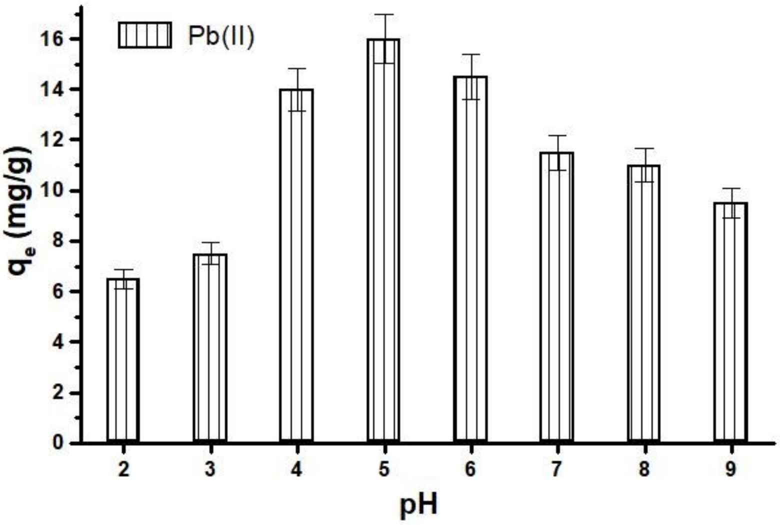

**Figure 6:** Effect of pH on adsorption of Pb(II) onto Cell-g-PAA (initial $Pb^{+2}$ conc. = 80 mg/L, adsorbent dose = 0.1 g, contact time = 60 min, batch volume = 25 mL).

**Effect of Initial Metal Ion Concentration**

In order to study the influence of initial metal ion concentration affecting the overall adsorption process, various batch adsorption experiments were carried out for different concentration in the range of 20 to 140 mg/L, keeping other parameters constant. The results are presented in Figure 7. The amount of Pb(II) adsorbed per unit mass of the adsorbent relatively increased with the increased in metal ion concentration from 20 up to 100 mg/L. However, at concentrations of 100 and 120 mg/L, the amount adsorbed was virtually the same. Having observed this, we concluded that the significant amount of Pb(II) adsorbed at higher concentration could be due to greater driving force at the liquid-solid interface, which consequently affect the mass transfer of the adsorbate from solution to adsorbent surface (31).

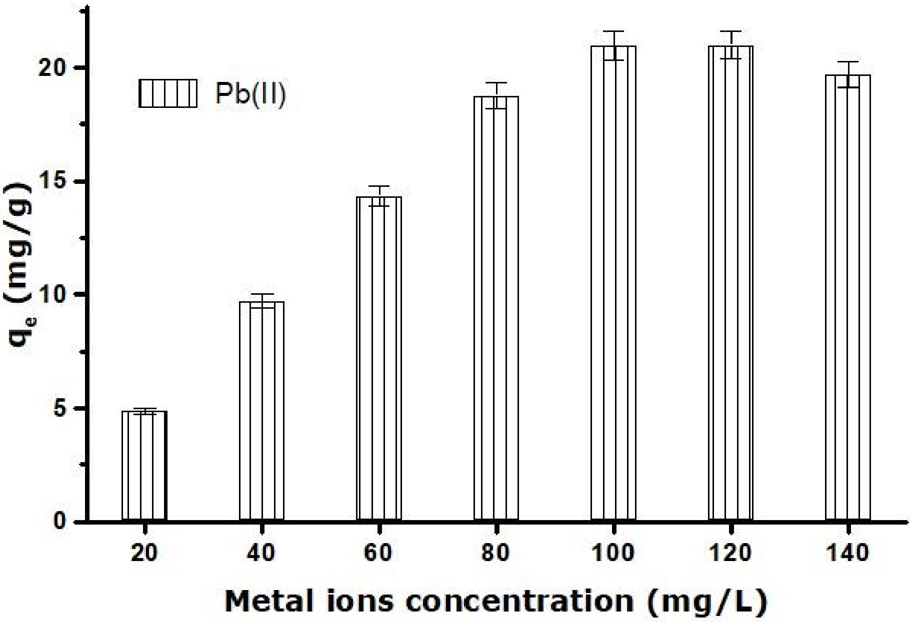

**Figure 7:** Effect of initial metal ion concentration on adsorption of Pb(II) onto Cell-g-PAA (initial pH = 5.0, adsorbent dose = 0.1 g, batch volume = 25 mL)

**Effect of Contact Time**

Figure 8 represents the results of equilibrium adsorption time and the adsorption capacity of the adsorbent. It was observed that the adsorption capacities increased steadily with the increased contact time from 5 to 60 minutes, and equilibrium point was attained after 45 mins for 20 mg/L concentration and 50 mins for 40 and 80 mg/L concentration. To ascertain the potential mechanism controlling the rate of adsorption, pseudo-first-order and pseudo-second-order were chosen to fit the experimental data. Table 2 showed the results of the kinetic models after simulations for different initial metal ion concentration. It was clear from the results that the adsorption kinetics followed pseudo-second-order model, with regression coefficients greater than 0.99 in all cases. Furthermore, calculated values of adsorption capacities agreed satisfactorily with the experimental data. Thus, chemisorption was assumed to be the rate-limiting step, indicating strong interactions due to the affinity of the adsorbent for the metal ion.

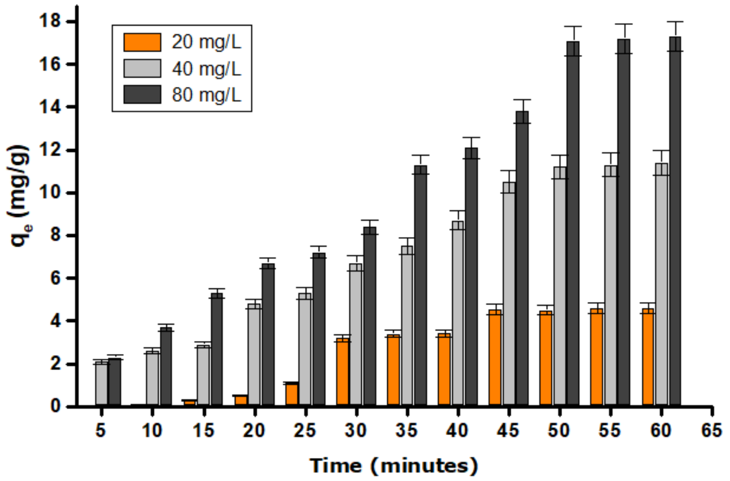

**Figure 8:** Effect of contact time on adsorption of Pb(II) onto Cell-g-PAA (initial Pb(II) conc. = 100 mg/L, pH = 5.0, adsorbent dose = 0.1 g)

**Table 2:** Rate constants and regression coefficients for adsorption Pb(II).

| **Pseudo-first-order model** | | | | | **Pseudo-second-order model** | | |
|---|---|---|---|---|---|---|---|
| Co (mg/L) | $q_{max\ exp}$ (mg/g) | $q_{max\ cal.}$ (mg/g) | $k_1$ (1/min) | $R^2$ | $q_{max\ cal.}$ (mg/g) | $k_2$ (g/mg/min) | $R^2$ |
| 20 | 3.81 | 1.63 | 0.008 | 0.711 | 3.75 | 0.091 | 0.996 |
| 40 | 11.30 | 5.25 | 0.007 | 0.882 | 10.90 | 0.084 | 0.999 |
| 80 | 17.62 | 10.31 | 0.005 | 0.912 | 16.43 | 0.075 | 0.998 |

**Analysis of Adsorption Isotherms**

Adsorption isotherm models are considered as the most versatile tools to understand adsorption patterns of adsorption systems. In this study, the Langmuir isotherm model was found to fit the experimental data well as illustrated in Figure 9. From the linear plots of the two isotherm models, all the adsorption parameters were determined as presented in Table 3. Based on regression coefficients ($R^2$) of the two models, Langmuir isotherm model described the adsorption process well with the calculated maximum adsorption capacity of 20.37 mg/g. Furthermore, separation factor ($R_L$) which is a dimensionless constant calculated was below unity; thus indicating the favorability of the adsorption. Langmuir adsorption model assumed homogenous distribution of adsorbate onto the adsorbent surface (monolayer coverage) (32).

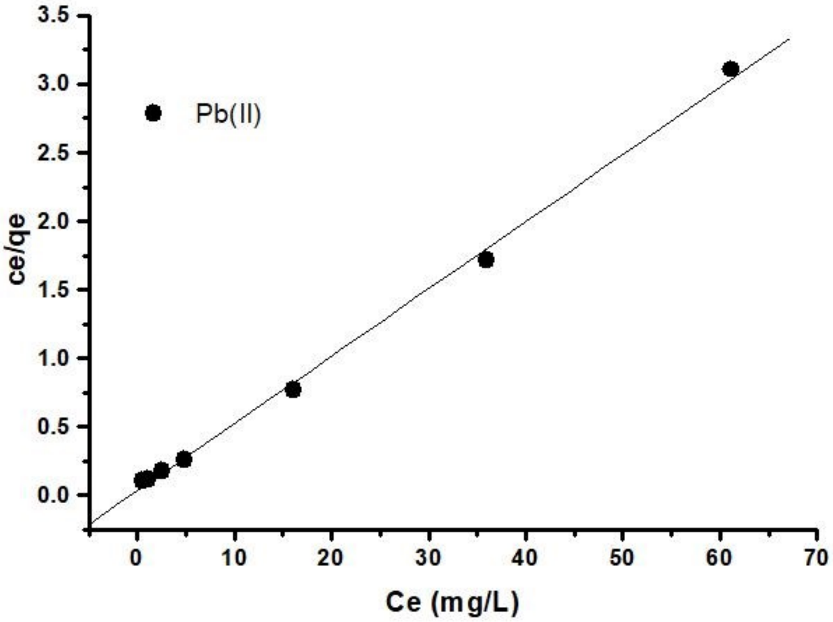

**Figure 9:** Langmuir isotherm plot for adsorption Pb(II) onto Cell-g-PAA.

**Table 3:** Isotherm constants and regression coefficients for adsorption of Pb(II)

| **Langmuir model** | | | | **Freundlich model** | | |
|---|---|---|---|---|---|---|
| $q_{max}$ (mg/g) | $R_L$ | $Q_L$ (L/mg) | $R^2$ | $K_F$ (mg/g) | *n* | $R^2$ |
| 20.37 | 0.004 | 0.821 | 0.998 | 1.09 | 20.40 | 0.739 |

## CONCLUSIONS

Sequestration of Pb(II) ions from aqueous solution was achieved by using a renewable, efficient, modified low-cost agricultural waste biomass. FTIR, SEM and XRD analyses of the grafted sample confirmed the grafting of polyacrylic acid onto cellulosic *Hyphaene thebaica* fiber. It has been observed that Pb(II) ions adsorption increased with an increase of the contact time and metal ion concentration until equilibrium was attained in 45 minutes but decreased at pH values above 6.0. Two popular adsorption isotherms and kinetic models were applied to test the applicability of the adsorption processes. The adsorption isotherm analysis is compatible with a Langmuir isotherm model which assumed monolayer adsorption process where as the kinetic mechanism indicated the prevalence of chemisorption. The study employed a green approach to the synthesis of the graft copolymer. The method is green because it requires less energy, less time, and less organic solvent consumption.

## ACKNOWLEDGEMENT

Financial support from the TETFund through the institutional-based research grant is gratefully acknowledged.

## REFERENCES

1. Qiu X, Hu S. Smart materials based on cellulose: a review of the preparations, properties and applications. Materials (Basel). 2013; 6:738-81.

2. Wei H, Rodriguez K, Renneckar S, Vikesland PJ. Environmental science and engineering applications of nanocellulose-based composites. Environ. Sci. Nano. 2014; 1(4):302-16.

3. Siro I, Plackett D. Microfibrillated cellulose and new nanocomposite materials: a review. Cellulose. 2014; 17(3): 459-94.

4. Plackett DV, Letchford K, Jackson JK, Burt HM. A review of nanocellulose as a novel vehicle for drug delivery. Nordic. Pulp Pap. Res. J 2014; 29(1): 131-41.

5. Gupta VK, Pathania D, Singh P, Rathore BS, Chauhan P. Cellulose acetate-zirconium (IV) phosphate nano-composite with enhanced photo-catalytic activity. Carbohydr. Polym. 2013; 95(1): 434-40.

6. Kumar R, Sharma RK, Singh AP. Cellulose based grafted biosorbents- Journey from lignocellulose biomass to toxic metal ions

sorption applications- A review. Journal of Molecular Liquids. 2017; 232: 62-93.

7. Zhang J, Wu J, Cao Y, Sang S, Zhang J, He J. Synthesis of cellulose benzoates under homogeneous conditions in an ionic liquid. Cellulose. 2009; 16(2): 299-308.
8. Wan Daud WR, Djuned FM. Cellulose acetate from oil palm empty fruit bunch via a one step heterogeneous acetylation. Carbohydr. Polym. 2015; 132: 252-60.
9. Stein A, Klemm D, Syntheses of cellulose derivatives via O-triorganosilyl cellulose I. Effective synthesis of organic cellulose esters by acetylation of trimethyl silyl celluloses. Die Makromolekulare Chemie Rapid Communications. 1988; 9(8): 569-73.
10. Bali G, Meng X, Deneff JI, Sun Q, Arthur JR. The effect of Alkaline pre-treatment methods on cellulose structure and Accessibility. ChemsusChem Communications. 2014; 2(3): 1-5.
11. Roy D, Semsarilar M, Guthriea JT, Perrier S. Cellulose modification by polymer grafting, A review. Chem. Soc. Rev. 2006; 38: 2046-64.
12. Mishra S, Usha GR, Sen G. Microwave initiated synthesis and application of polyacrylic acid grafted carboxymethyl cellulose. Carbohydr. Polym. 2011; 87: 2255-62.
13. Nada AAMA, Alkady MY, Fekry HM. Synthesis and characterization of grafted cellulose for use in water and metal ions sorption. Bioresources. 2008; 3:46-59.
14. Hajeeth T, Sudha PN, Vijayalakshmi TG. Sorption studis on Cr(VI) removal from aqueous solution using cellulose grafted with acrylonitrile monomer. Int. J. Biol. Macromol. 2014; 66:295-301.
15. Okieimen FE, Sogbaike CE, Ebhoaye JE. Removal of cadmium and copper ions from aqueous solution with cellulose graft copolymers. Sep. Purif. Technol. 2005; 44: 85-89
16. Salisu A, Mohd MS, Ahmedy AN, Ibrahim WAW, Khairil JA. Removal of lead ions from aqueous solutions using sodium alginate-graft-poly(methyl methacrylate) beads. Desal. Water Treat. 2016; 57(33): 15353- 61.
17. Naseem R, Tahir SS. Removal of Pb(II) from aqueous solution by using bentonite as an adsorbent. Water Res. 2001; 35: 3982-6.
18. Salisu A, Mohd MS, Ahmedy AN, Ibrahim WAW, Khairil JA. Alginate graft polyacrylonitrile beads for the Removal of lead ions from aqueous solutions Polym Bull. 2016; 73: 519-37.
19. Raji C, Anirudhan TS. Batch Cr(VI) removal by polyacrylamide-grafted sawdust: kinetics and thermodynamics. Water Res. 1998; 32: 3772-80.
20. Sharma S, Pathania D, Singh . Preparation, characterization and Cr(VI) adsorption behavior study of poly(acrylic acid) grafted Fiscus carica bast fiber. Adv. Mater. Lett. 2013; 4: 271-6.
21. Rani P, Sen G, Mishra S, Jha U. Microwave assisted synthesis of polyacrylamide grafted gum ghatti and its application as flocculant. Carbohydr. Polym. 2012; 89: 275-81.
22. Isiklan N, Kursun F, Inal M. Graft copolymerization of itaconic acid onto sodium alginate using benzoyl peroxide. Carbohydr. Polym. 2010; 101: 665-72.
23. Langmuir I. The adsorption of gases on plane surfaces of glass, mica and platinum. J. Chem. Soc. 1918; 40: 1361-403.
24. Freundlich HMF. Uber die adsorption in losungen. Zeitschrift fur physikalische. chemie (Leipzig). 1906; 57A, 385-470.
25. Gurgel LV, Gil LF. Adsorption of Cu(II), Cd(II) and Pb(II) from aqueous single solution by succinylated twice-mercerized sugarcane bagasse functionalized with triethylenetetraamine. Water Res. 2009; 43:4479-88.
26. Ho YS, McKay G. Pseudo-second-order model for sorption processes. Proc. Biochem. 1999; 34: 451-465.
27. David WJ, Hudson SM. Review of vinyl graft copolymerization featuring recent advances toward controlled radical-based reactions and illustrated with chitin/chitosan trunk polymers. Chem. Rev. 2001; 101: 3245-73.
28. Umar A, Mohd MS, Salisu A, Ibrahim WAW, Khairil AJ, Abdul Keyon AS. Preparation and characterization of starch grafted with methaacrylamide using ammonium persulphate initiator. Materials letters. 2016; 185: 173-6.
29. Arowona MT, Olatunji GA, Saliu OD, Adeniyi OR, Atolani O, Adisa MJ.

Thermally stable rice husk microcrystalline cellulose as adsorbent in PTLC plates. JOTCSA. 2018; 5(3): 1177-84.

30. Gupta VK, Agarwal S, Singh P, Pathania D. Acrylic acid grafted cellulosic Luffa cylidrical fiber for the removal of dye and metal ions. Carbohydr. Polym. 2013; 98: 1214-21.

31. Zhou Q, Yan C, Luo W. Preparation of a novel carboxylate-rich wheat straw through surface graft modification for efficient separation of Ce (III) from wastewater. Materials and Design. 2016; 97: 195-203.

32. Dang V, Doan HD, Dang-Vu AL. Equilibrium and kinetics of biosorption of cadmium (II) ad copper (II) ions by wheat straw. Bioresource Technol. 2008; 100: 211-19.